トレーサビリティーシステム開発

・輸入業者の協力を得て、輸入動物の国内分布に関するトレーサビリティーシステムを開発した。パソコン用オンラインシステムで有効性を確認

ハムスターの輸入動物に関しては1カ月後、3カ月後に販売実績・流通先（地域）を再入力
流通先は50%が関東、17.6%が関西、3.7%が中部、他地域は1%（380件、4万頭登録）

疫学調査と危害情報提供

・関西、関東の港湾労働者に関する動物由来感染症の疫学調査

3713名（関東2186名、関西1527名）の血清調査の結果11名がHFRS抗体陽性

・輸入業者のレプトスピラ感染と原因動物の同定

静岡県の輸入業者2名が、原因不明の発熱、多臓器障害で入院

動物輸入の実績調査（研究班で一部買い上げ）、レプトスピラ症を疑う

患者と買い上げ動物（アメリカモモンガー）のレプトスピラが同一であることの証明

在庫アメリカモモンガーの処分

・動物園動物および飼い犬における結核の感染事例についての情報提供

関西、関東の動物園における人型結核のサル類での流行（2004、2005年）

ミニチュアダックスフンド（2004）（♂・3歳9ヶ月）結核患者から飼い犬への感染
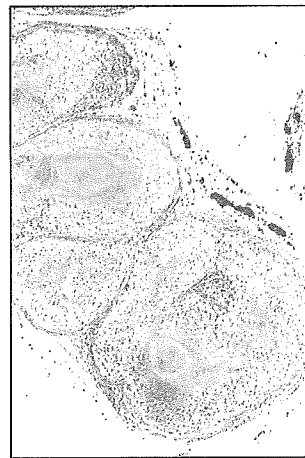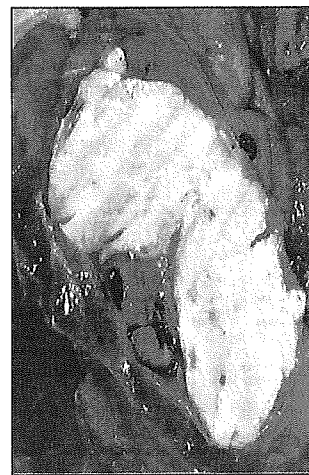
基盤研究（サル類）

- 霊長類における感染症の発生調査

  （動物園でのトキソプラズマ症、エルシニア症など）

- 血清抗体を用いたBウイルスとHSVの新しい鑑別診断法の確立
  - Bウイルスゲノム：PCRマイクロプレート・ハイブリダイゼーション法（PMH）の確立
  - 三叉神経節での潜伏感染の把握
  - 三叉神経潜伏ウイルスゲノムコピーの定量
  - 潜伏ウイルスゲノム解析

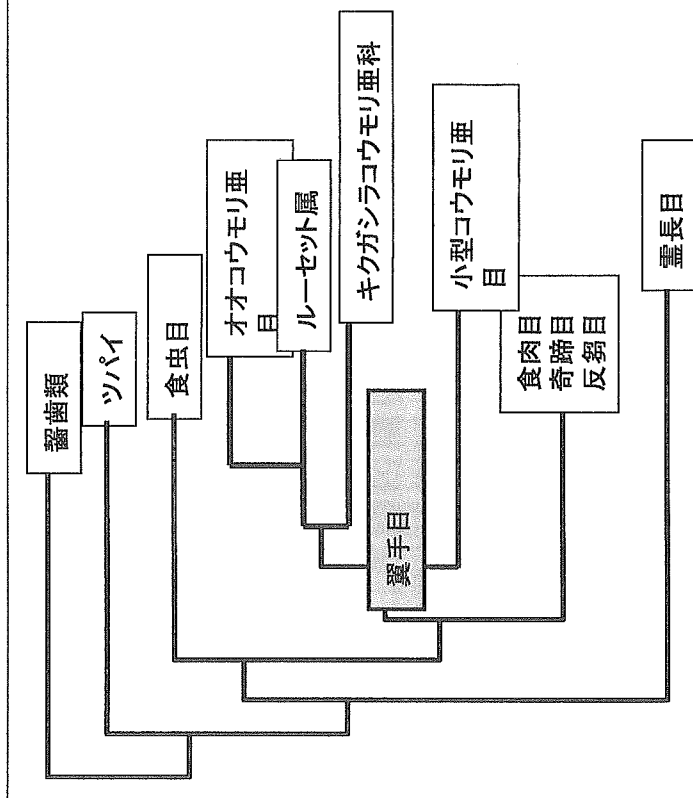- 組換え抗原（gG）を用いた抗体の鑑別診断

カニクイザル三叉神経節潜伏Bウイルスゲノムコピー数（log10）

No.	ID	Sex	BW(kg)	Right TG	Left TG
B2	96C0527	M	2.90	5.6	5.8
B3	97C0123	M	3.05	5.3	ー
B4	96C0389	M	2.45	6.2	ー
B9	96C0115	M	3.10	4.9	6.4
B12	96C0220	F	2.90	4.8	ー
B14	96C0384	F	2.60	5.9	5.2
B16	96C0296	F	2.65	6.3	6.6

基盤研究（翼手目）

基盤研究

・翼手目：海外との共同研究

　翼手類の分布、生理特性、免疫機能、初代培養細胞、免疫血清、抗体測定（ELISA）法

オオコウモリの体温変動（6℃）

ミトコンドリアDNAから見た系統樹

翼手目は1系統。ルーセット属は両亜目のミッシングリンクか？
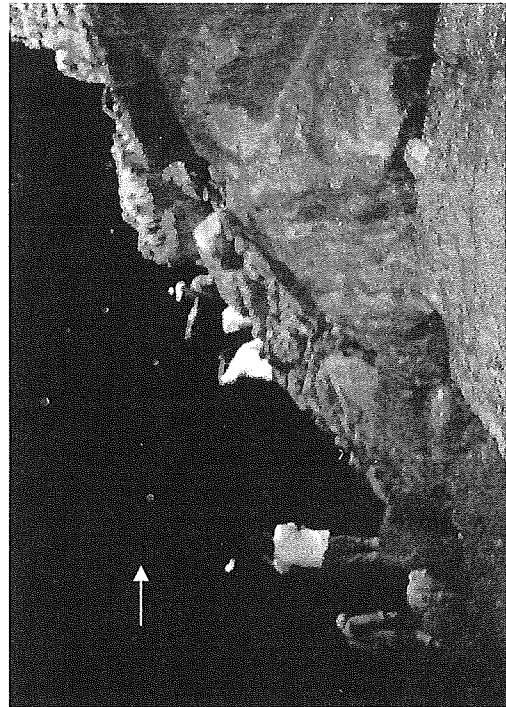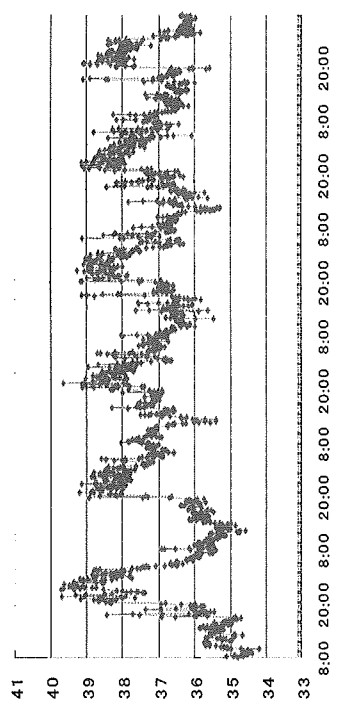
CBBstain　　WB by anti-IgG

whole IgG　　WB by anti-IgG
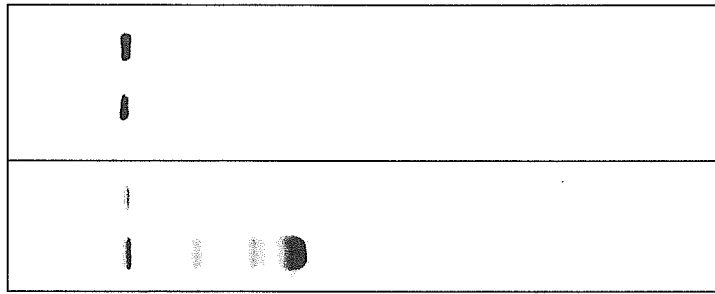
whole IgG　whole　IgG
Serum　　　serum

基盤研究（齧歯類）

・輸入齧歯類の病原体調査：

　ペスト、野兎病、レプトスピラ、ライム病、HFRS、LCM、寄生虫について検査
　レプトスピラ(10〜50%)、ライム病(20.6%)、寄生虫は陽性、
　LCM、HFRS、野兎病は陰性

基盤研究（ウイルス出血熱等の診断）

| 疾病	抗体検出 遺伝子組換え・合成抗原	抗原検出 抗原キャプチャー	鑑別診断 MoAb
マールブルグ病	○	○	
エボラ出血熱			
レストン株	○	○	○
ザイール株	○	○	○
スーダン株	○	○	○
ラッサ熱	○		
クリミアコンゴ出血熱	○		
HFRS、LCM	○		
アルゼンチン出血熱	○		

リスクコミュニケーション（成果の発表）

・ 厚労省研修会、都民講座、市民講座、NHKなどで動物由来感染症について教育・啓蒙

・ 獣医学会、獣医師会、実験動物学会、公衆衛生学会、感染症学会などで講演、

・ 国際学会、国際獣医デー等で講演

・ 新聞紙上連載

研究組織

主任研究者
吉川 泰弘・東大院農学生命科学研究科

分担研究者
内田 幸憲・厚労省神戸検疫所
本藤 良・日本獣医畜産大学獣医公衆衛生
大田 周司・厚労省東京検疫所 川崎支所
森川 茂・厚労省 国立感染症研究所
宇根 有美・麻布大学獣医学部

協力研究者
大松 勉・東大院農学生命科学研究科
鈴木 荘介・厚労省神戸検疫所
中島 健介・厚労省 国立感染症研究所
今成 敏夫・厚生省 成田検疫所
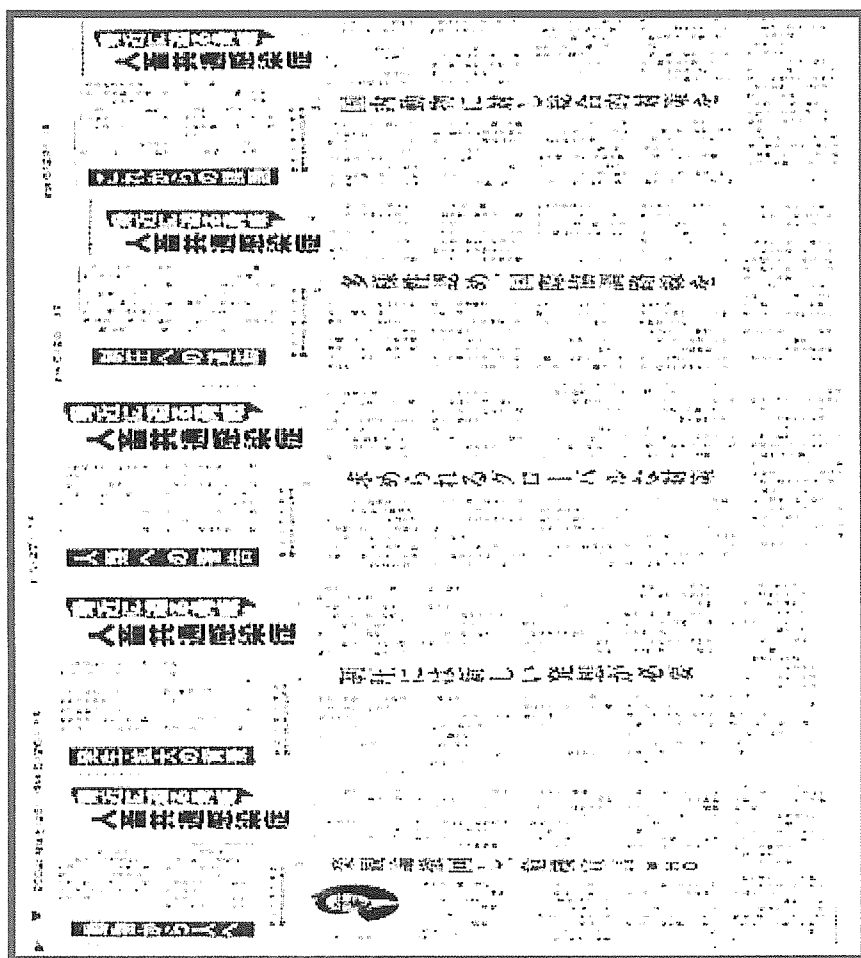
資料・業績

Inhibition of cell proliferation by SARS-CoV infection in Vero E6 cells

Tetsuya Mizutani[1], Shuetsu Fukushi[1], Daisuke Iizuka[2], Osamu Inanami[2], Mikinori Kuwabara[2], Hideaki Takashima[3], Hiroshi Yanagawa[3], Masayuki Saijo[1], Ichiro Kurane[1] & Shigeru Morikawa[1]

[1]Special Pathogens Laboratory, Department of Virology 1, National Institute of Infectious Diseases, Tokyo, Japan; [2]Laboratory of Radiation Biology, Department of Environmental Veterinary Sciences, Graduate School of Veterinary Medicine, Hokkaido University, Sapporo, Japan; and [3]Department of Biosciences and Informatics, Faculty of Science and Technology, Keio University, Yokohama, Japan

Abstract

Severe acute respiratory syndrome (SARS) is caused by SARS-coronavirus (SARS-CoV). Infection of Vero E6 cells with SARS-CoV inhibits cell proliferation. Our previous study indicated that Akt, which is poorly phosphorylated in confluent cultures of Vero E6 cells, is phosphorylated and then dephosphorylated upon infection by SARS-CoV. In the present study, we showed that a serine residue of Akt was phosphorylated in Vero E6 cells in subconfluent culture and that Akt was dephosphorylated rapidly after SARS-CoV infection without up-regulation of its phosphorylation. Phosphorylation of glycogen synthase kinase-3β, which is one of the downstream targets of Akt, was prevented in SARS-CoV-infected cells. However, treatment with glycogen synthase kinase-3β small interfering RNA indicated that the glycogen synthase kinase-3β signaling pathway was not related to inhibition of cell proliferation. Treatment of Vero E6 cells with the phosphatidylinositol 3'-kinase/Akt inhibitor, LY294002, which induces dephosphorylation of Akt, inhibited cell proliferation. As shown in our previous studies, apoptosis occurred in virus-infected cells within 18 h postinfection. Cellular mRNA transcription, which was reported to be up-regulated in SARS-CoV-infected Caco-2 cells, was not up-regulated in virus-infected Vero E6 cells, partially as a result of apoptosis. These results suggested that inhibition of cell proliferation is regulated by both the phosphatidylinositol 3'-kinase/Akt signaling pathway and by apoptosis in SARS-CoV-infected Vero E6 cells. This is the first study to analyze SARS-CoV-induced cell growth inhibition.

Introduction

Severe acute respiratory syndrome (SARS) is a newly discovered infectious disease caused by a novel coronavirus, SARS coronavirus (SARS-CoV) (Marra, 2003; Rota, 2003). SARS spread from Guangdong province in China to more than 30 countries in late 2002, causing severe outbreaks of atypical pneumonia. Because both the virulence and the mortality rate of this virus are very high, it is important to understand the mechanisms of pathogenesis of SARS-CoV infection for the prevention of SARS.

Our recent studies indicated that signaling pathways are activated upon infection of confluent cultures of Vero E6 cells with SARS-CoV (Mizutani *et al.*, 2004a,b,c). Mitogen-activated protein kinases (MAPKs), including p38, c-Jun N-terminal protein kinase (JNK) and extracellular signal-related kinase (ERK) 1/2, and their MAPKKs, are activated in SARS-CoV-infected Vero E6 cells (Mizutani *et al.*, 2004b). In particular, p38 is involved in induction of apoptosis

because a p38 inhibitor was shown to partially prevent apoptosis induced by SARS-CoV infection. Signal transducer and activator of transcription (STAT)-3, which is ordinarily phosphorylated at a tyrosine residue in Vero E6 cells, is dephosphorylated by SARS-CoV-induced activation of p38 (Mizutani *et al.*, 2004a). Akt, which has important antiapoptotic roles, is first phosphorylated at a single serine residue shortly after SARS-CoV infection, and subsequently dephosphorylated during the course of viral infection (Mizutani *et al.*, 2004c). However, threonine phosphorylation of Akt is not detected, and glycogen synthase kinase (GSK)-3β, which is a downstream target of Akt, is slightly phosphorylated in virus-infected cells, suggesting that Akt is unable to prevent virus-induced apoptosis. Interestingly, both Akt and JNK signaling pathways are important for establishing persistent SARS-CoV infection of Vero E6 cells (Mizutani *et al.*, 2005). The weak activation of Akt in cloned Vero E6 cells cannot allow escape from SARS-CoV-induced apoptosis. Thus, the signaling pathway of apoptosis is stronger than

the antiapoptotic pathway in virus-infected Vero E6 cells. Recent studies showed that expression of nucleocapsid, X1, and spike proteins of SARS-CoV can induce apoptosis in cells (He *et al.*, 2003; Surjit *et al.*, 2004; Chang *et al.*, 2004; Tan *et al.*, 2004). Interestingly, nucleocapsid protein induced apoptosis into COS-1 cells in the absence of growth factors, and both JNK and p38 MAPK were up-regulated in nucleocapsid expressing cells, whereas ERK1/2 and Akt were down-regulated (Surjit *et al.*, 2004).

Akt activated by phosphatidylinositol 3′-kinase (PI3K) regulates cell proliferation, the cell cycle and cell survival. A number of proteins, such as Bad, caspase-9 and GSK-3β, have been identified as downstream targets of Akt (Cardone *et al.*, 1998; Pap & Cooper, 1998; Vanhaesebroeck & Alessi, 2000). These proteins are inactivated when phosphorylated by Akt. Activation of Akt by infection with a number of viruses has been reported previously. LMP-1 protein of Epstein–Barr virus has been shown to bind to the p85 subunit of PI3K, resulting in activation of both PI3K and Akt (Dawson *et al.*, 2003). The middle T antigen of murine polyomavirus and the X protein of hepatitis B virus also bind to the p85 subunit of PI3K, leading to activation of Akt (Whitman *et al.*, 1985; Dahl *et al.*, 1998; Lee *et al.*, 2001). Activation of the PI3K/Akt signaling pathway by a variety of viruses is thought to be involved in the establishment of latent and chronic infections by allowing virus-infected cells to escape from apoptosis. Activation of the PI3K/Akt signaling pathway may lead to a delay in apoptosis of host cells, and the virus life cycle might be completed before apoptotic cell death of the host cells. Subsequent apoptosis facilitates the spread of the virus (Roulston *et al.*, 1999). As described above, the PI3K/Akt signaling pathway also promotes cell proliferation. Mirza *et al.* (2004) reported that the PI3K/Akt signaling pathway cooperates with the ERK signaling pathway to promote cell cycle progression in both normal and cancer cells. GSK-3β is a ubiquitously expressed protein-serine/threonine kinase and its activity is inhibited by Akt phosphorylation (Cross *et al.*, 1995). In addition, GSK-3 is now a well-known key component in a large number of cellular processes and disease states, including p53, hypoxia, prions and endoplasmic reticulum stress (Loberg *et al.*, 2002; Song *et al.*, 2002; Watcharasit *et al.*, 2002; Perez *et al.*, 2003). The effects of activation of GSK-3β are mediated through phosphorylation and proteolytic turnover of cyclin D1 (Diehl *et al.*, 1998), resulting in the induction of cell cycle arrest via prevention of retinoblastoma tumor suppressor protein (Rb) hyperphosphorylation.

In the present study, we found that cell proliferation was completely abolished when growing Vero E6 cells were infected with SARS-CoV. Furthermore, we showed that Akt was dephosphorylated without any increase in its phosphorylation upon SARS-CoV infection in subconfluent cultures of Vero E6 cells, in contrast to the tentative up-regulation of

phosphorylation of Akt prior to dephosphorylation in confluent cultures of these cells. In our previous study, we showed that caspase-3, which is one of the key factors in apoptosis, was activated within 18 h postinfection (p.i.) in virus-infected cells. Thus, both acute dephosphorylation of Akt and apoptotic events are likely to contribute to the inhibition of cell proliferation of SARS-CoV infected Vero E6 cells.

Materials and methods

Cells and virus

Vero E6 cells were subcultured routinely in 75-cm^3 flasks in Dulbecco's modified Eagle's medium (DMEM) (Sigma, St Louis, MO) supplemented with 0.2 mM L-glutamine, 100 units mL^{-1} penicillin, 100 μg mL^{-1} streptomycin, and 5% (volume in volume, v/v) fetal bovine serum (FBS), and maintained at 37 °C in an atmosphere of 5% CO_2. For use in the experiments, the cells were split once on to 6-, 24- and 96-well tissue culture plate inserts and cultured until they reached 30% or 100% confluence (referred to as subconfluent and confluent, respectively). In the case of subconfluent cell culture, DMEM containing 5% FBS was used. The PI3K inhibitor, LY294002 (Cell Signaling Technology Inc., Beverly, MA), was dissolved in dimethyl sulfoxide (DMSO) at a concentration of 10 mM. DMSO alone was used as a control. SARS-CoV, which was isolated as Frankfurt 1 and kindly provided by Dr. J. Ziebuhr, was used in the present study. Infection was usually performed at a multiplicity of infection of 10.

Western blotting

After virus infection, whole-cell extracts were electrophoresed on either 10% or 10–20% gradient polyacrylamide gels, and transferred electrophoretically onto polyvinylidene fluoride (PVDF) membranes (Immobilon-P, Millipore, Bedford, MA). In the present study, we applied two sets of samples to polyacrylamide gels, and the membranes were either divided into two halves after blotting using a Proto-Blot II AP system (Promega Co., Madison, WI), or they were examined once using a LumiGLO Elite chemiluminescent system (Kirkegaard and Perry Laboratories, Gaithersburg, ML) and then stripped using Restore western blot stripping buffer (Pierce, Rockford, IL) for second detection. The following antibodies, obtained from Cell Signaling Technology Inc., were used in the present study at a dilution of 1 : 1000: rabbit antiphospho Akt (Ser473), rabbit antiphospho Akt (Thr308), rabbit anti-Akt, rabbit antiphospho GSK-3αβ rabbit antiphospho GSK-3β, rabbit anti-GSK-3β, rabbit antiphospho STAT3 (Tyr-705) antibody, rabbit antiphospho STAT3 (Ser-727) antibody, rabbit anti-p38 MAPK (Thr180/Tyr182) antibody, rabbit anti-p38 MAPK antibody,

rabbit antiphospho p44/42 MAPK (Thr202/Tyr204) (= ERK1/2) antibody, rabbit anti-p44/42 MAPK (= ERK1/2) antibody, rabbit antiphospho SAPK/JNK (Thr183/Tyr185) antibody, rabbit antiphospho Rb (Ser795), rabbit antiphospho Rb (Ser807/811) and mouse anti-Rb monoclonal antibody. Mouse anti-STAT3 antibody (diluted 1 : 2500) was obtained from BD Biosciences (Franklin Lakes, NJ). Mouse anti-β-Actin antibody was purchased from Sigma and used at a dilution of 1 : 5000. Rabbit anti-SARS nucleocapsid and membrane antibodies were described previously (Mizutani *et al.*, 2004b).

In vitro GSK-3 activation assay

Vero E6 cells were treated with or without epidermal growth factor (EGF) and LY294002 for 10 min, and then cell extracts were obtained using the lysis buffer supplied in the Akt kinase assay kit (Cell Signaling Technology Inc.). Selective immunoprecipitation of Akt was performed using immobilized Akt antibody. After incubation of immunoprecipitated Akt in kinase buffer containing GSK-3β fusion protein and ATP, GSK-3β phosphorylation was analyzed by western blotting using antiphospho GSK-3αβ antibody.

siRNA against GSK-3β

Both GSK-3β small interfering RNA (siRNA) and control siRNA were purchased from Santa Cruz Biotechnology (Santa Cruz, CA). Each siRNA (final concentration 100 nM) was transfected into 30% confluent Vero E6 cells in 96-well plates using the Magnetofection system (OZ Biosciences, Marseille, France) combined with FuGene 6 transfection reagents (Roche, Indianapolis, IL). Efficiency of transfection was determined using fluorescein-labeled Luciferase GL2 duplex (Dharmacon, Lafayette, CO), and we usually obtained nearly 100% transfection efficiency.

RT-PCR

Vero E6 cells were inoculated with SARS-CoV at a multiplicity of infection of 10. Total RNA was extracted from SARS-CoV-infected cells at 24 h p.i. and from mock-infected cells with Isogen (Nippon Gene, Tokyo, Japan). RNAs were reverse-transcribed using SuperScript III (Invitrogen, Carlsbad, CA) and random primers. Semiquantitative PCR amplification was performed using High Fidelity Platinum Taq DNA polymerase (Invitrogen) for 15 to 35 cycles. PCR primers were determined based on sequences with the accession numbers given in the report by Cinatl *et al.* (2004). Primers used in this study were for eukaryotic translation initiation factor 3, subunit 6 (forward 5′-TAATGCAATTCAGACAATGTGTCC-3′, reverse 5′-CTTCT GGAGTCATGTTCAATTTATCTGCC-3′), glyceraldehyde-3-phosphate dehydrogenase (GAPDH) (forward 5′-TGATG

ACATCAAGAAGGTGG-3′, reverse 5′-AGCTAGCTAATAG GACTCACTATAGGGTTACTCTCCTTGGAGGCCATGT-3′ including promoter sequence of T7 RNA polymerase), Ets variant gene 5 (forward 5′-CATGGCTACTCTTGGGAACC ACCCGGCC-3′, reverse 5′-ATGTACAACTCAGGTGCAAA TGTTCC-3′), zinc finger protein 384 (forward 5′-CTCTCT CCTTCTCTGCCTACAAAGACCC-3′, reverse 5′-GAAATG GTTACAACAAAGATGGCC-3′), core promoter element-binding protein (forward 5′-GCCGGGAGCCACGGGATTG GGCC-3′, reverse 5′-CGTTTACCTGTTGCCAGTACTCCT CC-3′), Von Hippel–Lindau syndrome (forward 5′-GAC GGCTGGCATGGTGGCTCCC-3′, reverse 5′-ACTCATGGC TCACTGCAGCCTCC-3′), transcription factor 8 (forward 5′-AACCTGTATGCTGTGATTCC-3′, reverse 5′-TCCCAAT TGTACAGCTTAAGAATAAACC-3′), trinucleotide repeat-containing 4 (forward 5′-TCAGCCACAGAGACCCTCCT CC-3′, reverse 5′-AGAAATTAAGAGAGAGAAAAAAATCC-3′), trichorhinophalangeal syndrome 1 (forward 5′-GCTTC AGTTTCATTGTTAACGGGCC-3′, reverse 5′-AAATATTG TTGTTTGGGGGAATCTCC-3′), inhibition of DNA-binding 4 (forward 5′-TATAGATAAATGAGTGACATTTCAT ACC-3′, reverse 5′-TTAAGGATCCAAGCATTTCCTCATCC C-3′), c-fos (forward 5′-CAGAGAGGAGAAACACATCTTC CC-3′, reverse 5′-GATACAATTTGAAAATATCCAGCACC-3′), Friend leukemia virus integration 1 (forward 5′-GACC-GAGTCGTCCATGTACAAGTACCC-3′, reverse 5′-AAAAC GTACAGCTTCTTTCTCAGAACC-3′), early growth response 1 (forward 5′-TGCAATTGTGAGGGACATGCTCA CC-3′, reverse 5′-AGCGCATTCAATGTGTTTATAAGCC-3′) and synoviral sarcoma, X breakpoint 4 (forward 5′-CT GTATTTTCTTGCAGTGTGCC-3′, reverse 5′-AACAGAGT GAGGGGGGCTTGACC-3′). The PCR products were confirmed to be of the correct sizes.

Results

Regulation of cell proliferation upon SARS-CoV infection

Mouse hepatitis virus (MHV), a prototype coronavirus, has been shown to arrest the cell cycle at G0/G1 phase (Chen *et al.*, 2004b). Therefore, we investigated whether SARS-CoV infection suppresses cell proliferation. Subconfluent Vero E6 culture cells were infected with SARS-CoV and the cell number was counted at 24 h p.i. As shown in Fig. 1(a,b), the number of virus-infected cells was not increased at 24 h p.i., whereas that of mock-infected cells was increased by 1.8-fold.

Dephosphorylation of a serine residue of Akt by SARS-CoV infection

As shown in our recent study (Mizutani *et al.*, 2004), a serine residue of Akt was phosphorylated from 8 to 18 h p.i. in

confluent Vero E6 cell cultures, and then dephosphorylated at 24 h p.i.; we concluded that Akt phosphorylation in SARS-CoV-infected cells had low activity (Mizutani *et al.*, 2004). Thus, phosphorylation followed by dephosphoryla-

tion of Akt occurred during the course of virus infection. However, it was still unclear whether virus infection was actually responsible for phosphorylation and/or dephosphorylation of Akt.

To investigate the phosphorylation level of Akt in growing Vero E6 cells, subconfluent cell cultures were used in the present study. As shown in Fig. 2b (mock infection lane), a serine residue of Akt was highly phosphorylated in subconfluent cultures. To examine whether the phosphorylated Akt was up- or down-regulated in subconfluent cell cultures upon SARS-CoV infection, a virus-infection time-course experiment was performed. Cells in subconfluent cultures were infected with the virus at a multiplicity of infection of 10 and western blot analyses were performed using antibodies to viral and cellular proteins at 7, 16 and 23 h p.i. Protein from mock-infected cells was obtained at 7 h. The time-dependent changes of (phospho-)protein level, such as viral nucleocapsid and membrane proteins, the kinetics of MAPKs, including p38, JNK and ERK 1/2, and STAT-3 in virus-infected subconfluent Vero E6 cells were similar to those in confluent cells after viral infection (Fig. 2a,b; Mizutani *et al.*, 2004b). As shown in Fig. 2a, only the kinetics of Ser473-phosphorylation of Akt were different. Akt, which was always phosphorylated in subconfluent cells, was dephosphorylated at 16 and 23 h p.i. On the other hand, Akt in mock-infected cells was continuously phosphorylated from 7 to 24 h p.i. (data not shown; Fig. 2c). We measured the
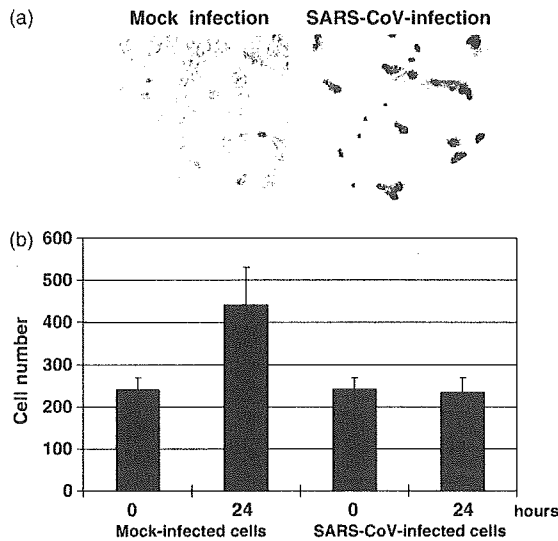

Fig. 1. Prevention of cell proliferation by severe acute respiratory syndrome coronavirus (SARS-CoV) infection. Subconfluent Vero E6 cells were infected with SARS-CoV at a multiplicity of infection of 10. Cell numbers of mock- and virus-infected cells were counted at 24 h postinfection.
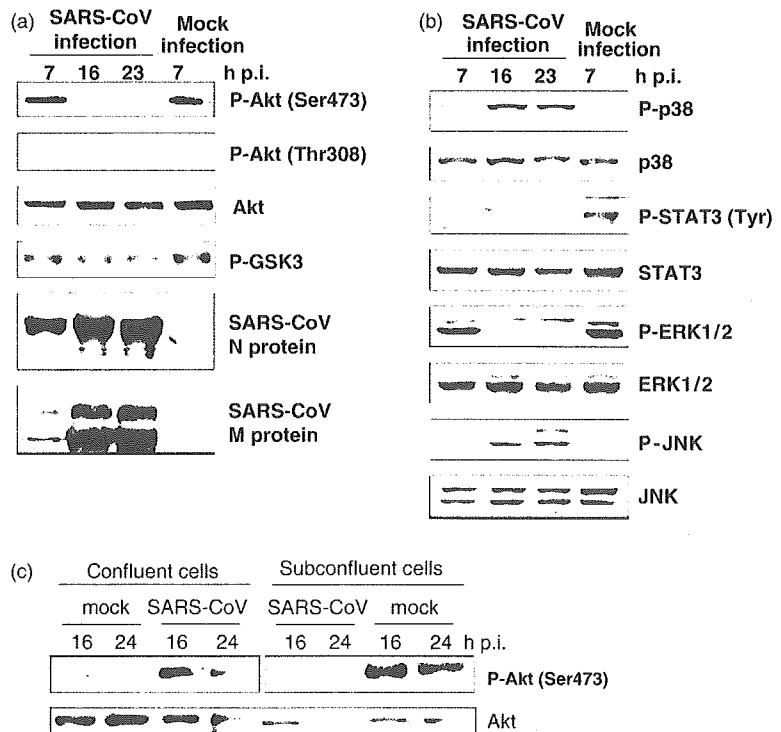
Fig. 2. Acute dephosphorylation of Akt serine by severe acute respiratory syndrome coronavirus (SARS-CoV) infection. (a,b) Subconfluent Vero E6 cells were infected with SARS-CoV at a multiplicity of infection of 10 and then western blot analysis was performed using anti-Akt, glycogen synthase kinase (GSK)-3β, viral proteins, p38, signal transducer and activator of transcription (STAT)3, extracellular signal-related kinase (ERK)1/2 and c-Jun nucleocapsid-terminal protein kinase (JNK) antibodies. (c) Confluent and subconfluent cells were infected with SARS-CoV at a multiplicity of infection of 10 and western blot analysis was performed. Proteins equivalent to same cell number were applied to the gel. p.i., postinfection.

densities of Ser473-phosphorylated Akt of mock-infected subconfluent cells and SARS-CoV-infected confluent cells at 16 h p.i. (Fig. 2c) using the LAS-3000 mini system (Fuji Photo Film Co. Ltd., Tokyo, Japan). The amount of phosphorylated Akt of mock-infected subconfluent cells was 4.8-fold higher than that of SARS-CoV-infected confluent cells. GSK-3β was also dephosphorylated in SARS-CoV-infected subconfluent cells. We next investigated whether Akt was phosphorylated in virus-infected subconfluent cell cultures before 7 h p.i. The phosphorylation level of Akt-serine was not up-regulated at 2, 4 or 6 h p.i. (data not shown). The phosphorylation of GSK-3 were also similar at 2 and 6 h p.i. (data not shown). In addition, phosphorylation level of Akt kinase did not significantly change from 7 to 23 h p.i. (data not shown). These results suggested that SARS-CoV infection induces dephosphorylation of a serine residue of Akt in subconfluent cultures, without tentative up-regulation of phosphorylation prior to dephosphorylation.

Activity of Akt in subconfluent cells

To investigate whether Akt serine phosphorylation represented a biologically active kinase in subconfluent cells, we examined the *in vitro* kinase activity of phosphorylated Akt. Subconfluent Vero E6 cells treated with EGF for 10 min or LY294002 for 1 h were lysed and Ser473-phosphorylated Akt in the cell lysate was precipitated with anti-Akt antibody. GSK-3β protein was added to the immunoprecipitated Akt with ATP, and western blotting was performed using antiphosphorylated GSK-3α/β antibody. As shown in Fig. 3, the level of phosphorylation of GSK-3 in EGF-treated cells was higher than that in nontreated cells. On the other hand, phosphorylation of GSK was not detected in cells treated with the PI3K inhibitor, LY294002. These results strongly suggested that Akt in subconfluent Vero E6 cell cultures was phosphorylated mainly at serine residues and had kinase activity.

Regulation of cell proliferation by Akt

The level of phosphorylated GSK-3β was decreased in virus-infected cells, possibly as a result of down-regulation of Akt
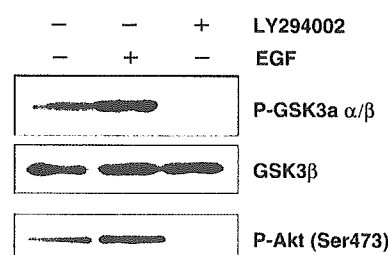

Fig. 3. Phosphorylation status of Akt in subconfluent cells. Epidermal growth factor and LY294002 were added to subconfluent Vero E6 cells for 10 min and 1 h, respectively. The cell lysates were precipitated using anti-Akt antibody. Glycogen synthase kinase (GSK)-3β protein was added to the immunoprecipitated Akt with ATP, and western blot analysis was performed using antiphosphorylated GSK-3α/β and anti-phosphorylated Akt (Ser) antibodies.

activation (Fig. 2a). Because one of the important roles of Akt is in cell cycle regulation by preventing GSK-3β-mediated phosphorylation and degradation of cyclin D1 (Diehl *et al.*, 1998), we examined whether GSK-3β regulates the proliferation of Vero E6 cells. Vero E6 cells were transfected with GSK-3β siRNA, and western blot analysis was performed 48 h later to detect the total amount of GSK-3β protein. As shown in Fig. 4a, the total amount of GSK-3β was reduced markedly by the siRNA, and the level of phosphorylated GSK-3β was reduced. However, GSK-3β siRNA-treated cells exhibited similar growth to those treated with control siRNA (Fig. 4b). The total amount of Rb and phosphorylated Rb was not affected by GSK-3β siRNA. The hyperphosphorylation form of Rb is known to be phosphorylated at least at Ser795, Ser807, and Ser811 (Faenza *et al.*, 2000; Jiang, 2002; Shibata & Nakamura, 2002), and hyperphosphorylation of Rb at Ser795 to release E2F is a critical step in the G1–S transition (Harbour & Dean, 2000).

We next investigated whether inhibition of the PI3K/Akt signaling pathway inhibits cell proliferation of Vero E6 cells. As shown in Fig. 5, complete inhibition by the PI3K inhibitor, LY294002, was observed at 48 h. We confirmed that serine residues of Akt were dephosphorylated in LY294002-treated cells in our previous study. These results
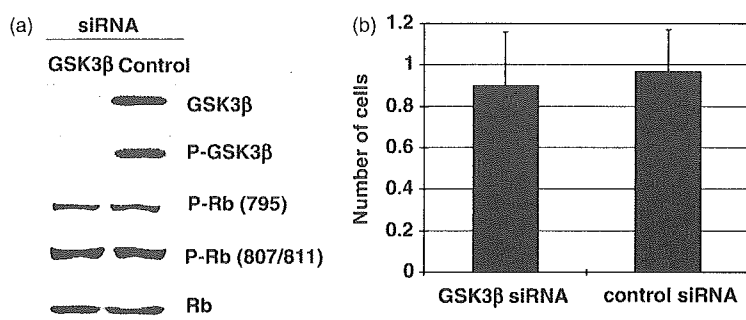

Fig. 4. Relationship between glycogen synthase kinase (GSK)-3β and Rb in cell proliferation. (a) GSK-3β small interfering RNA (siRNA) was transfected into subconfluent Vero E6 cells for 48 h and then western blot analysis was performed. (b) Cell number was determined using a WST-1 cell counting kit (Dojin, Kumamoto, Japan).

suggested that activation of Akt in subconfluent Vero E6 cells plays important roles in cell proliferation, and that down-regulation of Akt activity in SARS-CoV-infected cells prevents cell proliferation.

Down-regulation of cellular mRNAs in virus-infected cells

Although LY294002 inhibits proliferation of Vero E6 cells, apoptotic cell death was not induced by treatment with this
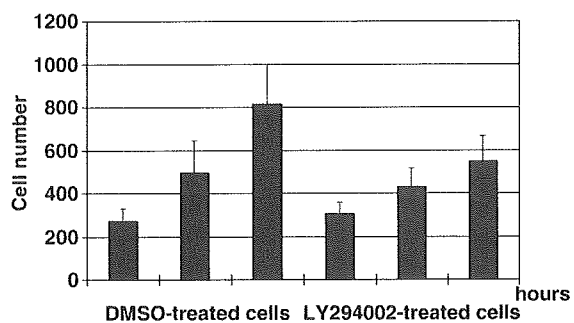

Fig. 5. Prevention of cell proliferation by LY294002 treatment. Subconfluent Vero E6 cells were treated with LY294002 at a concentration of 10 μM. Cell numbers of mock- and LY294002-treated cells were counted at 24 and 48 h postinfection.

agent (10 μM) for 48 h by western blot analysis using anti-cleaved caspase-3 (data not shown). As indicated in our previous study, apoptotic events progress in virus-infected cells. Therefore, these findings strongly suggested that both events Akt-dephosphorylation and apoptosis are responsible for the inhibition of cell proliferation in SARS-CoV-infected cells. We feel that transcriptional activity in virus-infected cells is important for understanding the viability of cells. Cinatl et al. (2004) demonstrated that SARS-CoV infection regulates cellular gene expression in a SARS-CoV-permissive cell line, Caco-2, at 24 h p.i. using high-density oligonucleotide arrays. We focused on up-regulated genes related to transfection factors, because several signaling pathways, which generally play important roles in the activation of transcription factors, are activated in SARS-CoV-infected Vero E6 cells. We selected 14 genes (including the housekeeping gene, GAPDH) that were shown previously to be up-regulated by several stimuli (Cinatl et al., 2004), and semi-quantitative reverse transcription PCR (RT-PCR) was performed using total RNA extracted from virus-infected confluent Vero E6 cells at 24 h p.i. The amount of total RNA was adjusted by the level of ribosomal RNA (Fig. 6s). Figure 6(b,c) shows genes that were down-regulated and that showed similar expression upon SARS-CoV-infection compared to mock-infected cells, respectively. Eukaryotic translation initiation factor 3, Ets variant gene 5, Zinc finger protein
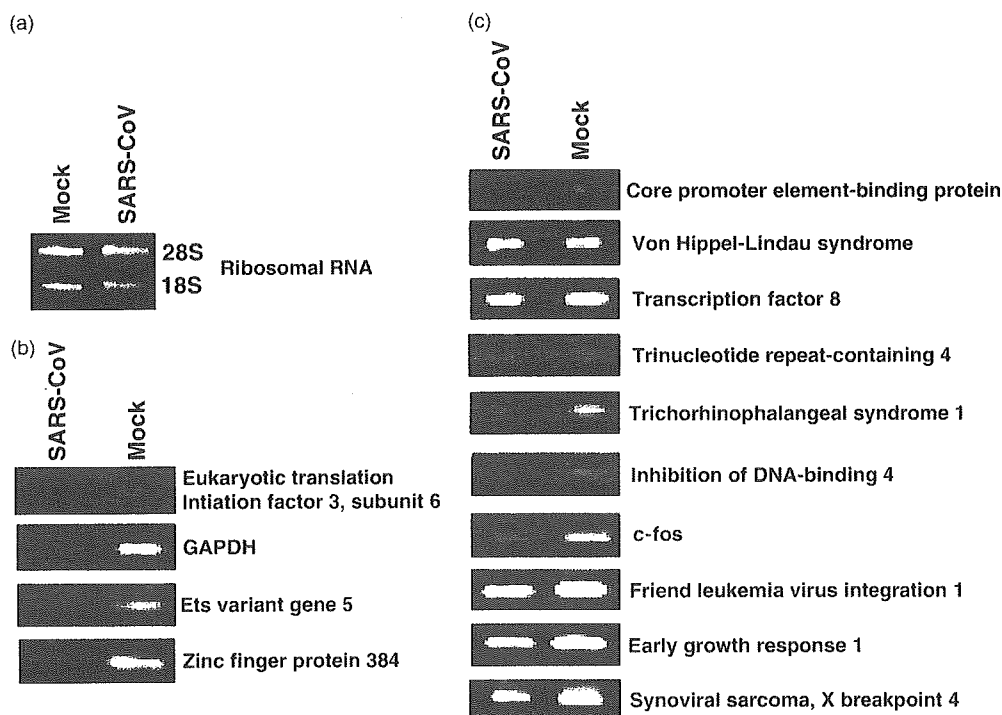

Fig. 6. Semiquantitative reverse transcription PCR (RT-PCR) of cellular transcripts. Total RNAs were extracted from virus-infected and mock-infected confluent Vero E6 cells at 24 h postinfection. Transcripts of cellular genes were assessed for their relative abundance by RT-PCR.

384 and GAPDH were down-regulated in SARS-CoV-infected cells. These results suggested that transcriptional shut-off occurred in particular (or in many) cellular mRNAs due to SARS-CoV infection, and that virus-infected cells are not proliferative due to Akt dephosphorylation and apoptosis.

Discussion

In the present study, we focused on the different kinetics of the phosphorylation status of Akt in subconfluent Vero E6 cells upon SARS-CoV infection. Akt-phosphorylation is up- and down-regulated by virus infection in the confluent cells, as shown in our previous report (Mizutani et al., 2004), but is down-regulated by virus infection in subconfluent cells. Therefore, one of the aims of the present study was to determine whether SARS-CoV has the potential for up- or down-regulation of Akt-phosphorylation in Vero E6 cells. Akt was phosphorylated in growing mock-infected cells (i.e. 30% confluency), whereas it was dephosphorylated in confluent cell cultures. An Akt-binding protein, carboxyl-terminal modulator protein (CTMP), is a well-known negative regulatory component of the Akt (Maira et al., 2001). CTMP, which binds to Akt, reduces the activity of Akt by inhibiting phosphorylation on serine and threonine residues. We found that the level of CTMP was below the limit of detection at 0–24 h p.i. in subconfluent virus-infected cells (data not shown), suggesting that dephosphorylation of Akt in subconfluent cell cultures upon viral infection was not regulated by CTMP. Although we obtained proteins from SARS-CoV-infected cells at different time points from 5 to 24 h p.i. in at least six experiments and performed western blot analysis using anti-phospho Akt (Ser) antibody, we were not able to find up-regulation of Akt-phosphorylation in SARS-CoV-infected subconfluent Vero E6 cells. Therefore, we concluded in this study that SARS-CoV has a potential of down-regulation of Akt-phosphorylation. It may be possible that SARS-CoV infection induces activation of Akt phosphatase(s).

In our previous study, we showed that apoptotic events, such as caspase-3 activation and DNA ladder formation, were detected in SARS-CoV-infected Vero E6 cells at 18 and 24 h p.i., respectively (Mizutani et al., 2004b,c). We could not find any up-regulated genes in SARS-CoV-infected Vero E6 cells, in contrast with SARS-CoV-infected Caco-2 cells, in which several genes were demonstrated to be up-regulated (Cinatl et al., 2004). This may have resulted from the faster progression of apoptosis and more rapid production of virus particles in infected Vero E6 as compared with Caco-2 cells. Thus, transcriptional shut-off in virus-infected cells may prevent cell proliferation with dephosphorylation of Akt.

In conclusion, the results of the present study suggested that SARS-CoV-infection affected Akt signaling pathways and gene expression. Down-regulation of Akt activity and the processing of apoptotic events in virus-infected cells may prevent cell proliferation. We assume that these phenomena are at least partly involved in the pathogenesis of SARS-CoV infection.

Acknowledgements

References

Cardone MH, Roy N, Stennicke HR, Salvesen GS, Franke TF, Stanbridge E, Frisch S & Reed JC (1998) Regulation of cell death protease caspase-9 by phosphorylation. Science 282: 1318–1321.

Chang YJ, Liu CY, Chiang BL, Chao YC & Chen CC (2004) Induction of IL-8 release in lung cells via activator protein-1 by recombinant baculovirus displaying severe acute respiratory syndrome-coronavirus spike proteins: identification of two functional regions. J Immunol 173: 7602–7614.

Chen CJ, Sugiyama K, Kubo H, Huang C & Makino S (2004) Murine coronavirus nonstructural protein p28 arrests cell cycle in G0/G1 phase. J Virol 78: 10410–10419.

Cinatl J Jr, Hoever G, Morgenstern B, Preiser W, Vogel JU, Hofmann WK, Bauer G, Michaelis M, Rabenau HF & Doerr HW (2004) Infection of cultured intestinal epithelial cells with severe acute respiratory syndrome coronavirus. Cell Mol Life Sci 61: 2100–2112.

Cross DAE, Alessi DR, Cohen P, Andjelkovich M & Hemmings BA (1995) Inhibition of glycogen synthase kinase-3 by insulin mediated by protein kinase B. Nature 378: 785–789.

Dahl J, Jurczak A, Cheng LA, Baker DC & Benjamin TL (1998) Evidence of a role for phosphatidylinositol 3-kinase activation in the blocking of apoptosis by polyomavirus middle T antigen. J Virol 72: 3221–3226.

Dawson CW, Tramountanis G, Eliopoulos AG & Young LS (2003) Epstein–Barr virus latent membrane protein 1 (LMP1) activates the phosphatidylinositol 3-kinase/Akt pathway to promote cell survival and induce actin filament remodeling. J Biol Chem 278: 3694–3704.

Diehl JA, Cheng M, Roussel MF & Sherr CJ (1998) Glycogen synthase kinase-3beta regulates cyclin D1 proteolysis and subcellular localization. Genes Dev 12: 3499–3511.

Faenza I, Matteucci A, Manzoli L, Billi AM, Aluigi M, Peruzzi D, Vitale M, Castorina S, Suh PG & Cocco L (2000) A role for

nuclear phospholipase Cbeta 1 in cell cycle control. *J Biol Chem* **275**: 30520–30524.

Harbour JW & Dean DC (2000) Rb function in cell-cycle regulation and apoptosis. *Nat Cell Biol* **2**: 65–67.

He R, Leeson A, Andonov A, *et al.* (2003) Activation of AP-1 signal transduction pathway by SARS coronavirus nucleocapsid protein. *Biochem Biophys Res Commun* **311**: 870–876.

Jiang JD, Denner L, Ling YH, *et al.* (2002) Double blockade of cell cycle at G1-S transition and M phase by 3-iodoacetamido benzoyl ethyl ester, a new type of tubulin ligand. *Cancer Research* **62**: 6080–6088.

Lee YI, Kang-Park S & Do SI (2001) The hepatitis B virus-X protein activates a phosphatidylinositol 3-kinase-dependent survival signaling cascade. *J Biol Chem* **276**: 16969–16977.

Loberg RD, Vesely E & Brosins FC III (2002) Enhanced glycogen synthase kinase-3beta activity mediates hypoxia-induced apoptosis of vascular smooth muscle cells and is prevented by glucose transport and metabolism. *J Biol Chem* **277**: 41667–41673.

Maira SM, Galetic I, Brazil DP, Kaech S, Ingley E, Thelen M & Hemmings BA (2001) Carboxyl-terminal modulator protein (CTMP), a negative regulator of PKB/Akt and v-Akt at the plasma membrane. *Science* **294**: 374–380.

Marra MA, Jones SJ, Astell CR, *et al.* (2003) The Genome sequence of the SARS-associated coronavirus. *Science* **300**: 1399–1404.

Mirza AM, Gysin S, Malek N, Nakayama K, Roberts JM & McMahonn M (2004) Cooperative regulation of the cell division cycle by the protein kinases RAF and AKT. *Mol Cell Biol* **24**: 10868–10881.

Mizutani T, Fukushi S, Murakami M, Hirano T, Saijo M, Kurane I & Morikawa S (2004a) Tyrosine dephosphorylation of STAT3 in SARS coronavirus-infected Vero E6 cells. *FEBS Lett* **577**: 187–192.

Mizutani T, Fukushi S, Saijo M, Kurane I & Morikawa S (2004b) Phosphorylation of p38 MAPK and its downstream targets in SARS coronavirus-infected cells. *Biochem Biophys Res Commun* **319**: 1228–1234.

Mizutani T, Fukushi S, Saijo M, Kurane I & Morikawa S (2004c) Importance of Akt signaling pathway for apoptosis in SARS-CoV-infected Vero E6 cells. *Virology* **327**: 169–174.

Mizutani T, Fukushi S, Saijo M, Kurane I & Morikawa S (2005) JNK and PI3K/Akt signaling pathways are required for establishing persistent SARS-CoV-infection in Vero E6 cells. *Biochim Biophys Acta* **1741**: 4–10.

Pap M & Cooper GM (1998) Role of glycogen synthase kinase-3 in the phosphatidylinositol 3-Kinase/Akt cell survival pathway. *J Biol Chem* **273**: 19929–19932.

Perez M, Rojo AI, Wandosell F, Diaz-Nido J & Avila J (2003) Prion peptide induces neuronal cell death through a pathway involving glycogen synthase kinase 3. *Biochem J* **372**: 129–136.

Rota PA, *et al.* (2003) Characterization of a novel coronavirus associated with severe acute respiratory syndrome. *Science* **300**: 1394–1399.

Roulston A, Marcellus RC & Branton PE (1999) Viruses and apoptosis. *Annu Rev Microbiol* **53**: 577–628.

Shibata Y & Nakamura T (2002) Defective flap endonuclease 1 activity in mammalian cells is associated with impaired DNA repair and prolonged S phase delay. *J Biol Chem* **277**: 746–754.

Song L, De Sarno P & Jope RS (2002) Central role of glycogen synthase kinase-3beta in endoplasmic reticulum stress-induced caspase-3 activation. *J Biol Chem* **277**: 44701–44708.

Surjit M, Liu B, Jameel S, Chow VT & Lal SK (2004) The SARS coronavirus nucleocapsid protein induces actin reorganization and apoptosis in COS-1 cells in the absence of growth factors. *Biochem J* **383**: 13–18.

Tan YJ, Fielding BC, Goh PY, Shen S, Tan TH, Lim SG & Hong W (2004) Overexpression of 7a, a protein specifically encoded by the severe acute respiratory syndrome coronavirus, induces apoptosis *via* a caspase-dependent pathway. *J Virol* **78**: 14043–14047.

Vanhaesebroeck B & Alessi DR (2000) The PI3K-PDK1 connection: more than just a road to PKB. *Biochem J* **346**: 561–576.

Watcharasit P, Bijur GN, Zmijewski JW, Song L, Zmijewska A, Chen X, Johnson GV & Jope RS (2002) Direct, activating interaction between glycogen synthase kinase-3beta and p53 after DNA damage. *Proc Natl Acad Sci USA* **99**: 7951–7955.

Whitman M, Kaplan DR, Schaffhausen B, Cantley L & Roberts TM (1985) Association of phosphatidylinositol kinase activity with polyoma middle-T competent for transformation. *Nature* **315**: 239–242.

Regulation of p90RSK phosphorylation by SARS-CoV infection in Vero E6 cells

Tetsuya Mizutani*, Shuetsu Fukushi, Masayuki Saijo, Ichiro Kurane, Shigeru Morikawa

Special Pathogens Laboratory, Department of Virology 1, National Institute of Infectious Diseases, Gakuen 4-7-1, Musashimurayama, Tokyo 208-0011, Japan
Department of Bacteriology 2, National Institute of Infectious Diseases, Gakuen 4-7-1, Musashimurayama, Tokyo 208-0011, Japan

Abstract The 90 kDa ribosomal S6 kinases (p90RSKs) are a family of broadly expressed serine/threonine kinases with two kinase domains activated by extracellular signal-regulated protein kinase in response to many growth factors. Our recent study demonstrated that severe acute respiratory syndrome (SARS)-coronavirus (CoV) infection of monkey kidney Vero E6 cells induces phosphorylation and dephosphorylation of signaling pathways, resulting in apoptosis. In the present study, we investigated the phosphorylation status of p90RSK, which is a well-known substrate of these signaling pathways, in SARS-CoV-infected cells. Vero E6 mainly expressed p90RSK1 and showed weak expression of p90RSK2. In the absence of viral infection, Ser221 in the N-terminal kinase domain was phosphorylated constitutively, whereas both Thr573 in the C-terminal kinase domain and Ser380 between the two kinase domains were not phosphorylated in confluent cells. Ser380, which has been reported to be involved in autophosphorylation by activation of the C-terminal kinase domain, was phosphorylated in confluent SARS-CoV-infected cells, and this phosphorylation was inhibited by SB203580, which is an inhibitor of p38 mitogen-activated protein kinases (MAPK). Phosphorylation of Thr573 was not upregulated in SARS-CoV-infected cells. Thus, in virus-infected cells, phosphorylation of Thr573 was not necessary to induce phosphorylation of Ser380. On the other hand, Both Thr573 and Ser380 were phosphorylated by treatment with epidermal growth factor (EGF) in the absence of p38 MAPK activation. Ser220 was constitutively phosphorylated despite infection. These results indicated that phosphorylation status of p90RSK by SARS-CoV infection is different from that by stimulation of EGF. This is the first detailed report regarding regulation of p90RSK phosphorylation by virus infection.
© 2006 Federation of European Biochemical Societies. Published by Elsevier B.V. All rights reserved.

Keywords: 90 kDa ribosomal S6 kinases; Phosphorylation; Severe acute respiratory syndrome

1. Introduction

The signaling pathway of extracellular signal-regulated kinase (ERK) regulates cellular processes, including growth, cell proliferation, survival, and motility [1]. The p90 ribosomal S6 kinases (RSK), a family of serine/threonine kinases, are impor-

tant substrates of ERK [2]. The RSK family consists of four isoforms (RSK1, 2, 3, and 4) and two structurally related RSK-like protein kinases (RLPK/MSK1) and RSK-B (MSK2) in humans [2–5]. Members of the RSK family contain two distinct kinase domains. The C-terminal kinase domain is thought to be involved in autophosphorylation at the critical step in 90 kDa ribosomal S6 kinase (p90RSK) activation [6–8]. On the other hand, the N-terminal kinase domain is capable of phosphorylation of substrates. Recent studies have clarified the mechanisms of activation of p90RSK. p90RSK1 is phosphorylated at Thr573 in the activation loop of the C-terminal kinase domain by ERK because the C-terminal of p90RSK has an ERK docking site [9,10]. Autophosphorylation at Ser380 in the linker region is thought to be induced by activation of the C-terminal kinase domain [11], and then PDK1 phosphorylates at Ser221 in the activation loop of the N-terminal kinase domain [12–14].

p90RSK is thought to have multiple functions. In quiescent cells, p90RSK is present in the cytoplasm, and p90RSK activated via the ERK signaling pathway by growth factors is imported into the nucleus. p90RSK activates nuclear factor-κB by phosphorylation of Iκ-B and phosphorylates the transcription factors, c-Fos and cAMP-response element-binding protein (CREB) [2]. It has been shown that p90RSK plays important roles in apoptosis and the cell cycle. p90RSK phosphorylates Bad [15,16] and C/EBPβ [17], which protects cells against apoptosis. Furthermore, p90RSK phosphorylates and inhibits Myt1, which is a p34cdc2 inhibitory kinase, resulting in G2 arrest in *Xenopus* extracts [18,19]. In mouse oocytes, Emi1 and p90RSK2 cooperate to induce metaphase arrest [20]. p90RSK also functions as a serum-stimulated Na^+/H^+ exchanger-1 kinase and regulates its activity [21]. Recently, it has been shown that p90RSK activation induces H_2O_2-mediated cardiac troponin I phosphorylation, which depresses the acto-myosin interaction and is important during the progression of heart failure [21]. Thus, p90RSK has been demonstrated to play key roles in regulating cellular functions in the ERK signaling pathway in vitro and in vivo.

Severe acute respiratory syndrome (SARS) is a newly discovered infectious disease caused by a novel coronavirus, SARS coronavirus (SARS-CoV) [22,23], which spread to more than 30 countries in late 2002, causing severe outbreaks of atypical pneumonia. Our recent studies using the monkey kidney cell line, Vero E6, demonstrated that a variety of signaling pathways are activated upon infection with SARS-CoV. Especially, p38 mitogen-activated protein kinase (MAPK) is thought to be involved in induction of apoptosis because a p38 inhibitor was

*Corresponding author. Fax: +81 42 564 4881.
E-mail address: tmizutan@nih.go.jp (T. Mizutani).

able to partially prevent cytopathic effects induced by SARS-CoV infection [24]. Signal transducer and activator of transcription (STAT)-3, which is ordinarily phosphorylated at a tyrosine residue, is dephosphorylated by SARS-CoV-induced activation of p38 [25]. c-Jun N-terminal protein kinase (JNK) and Akt are important for establishing persistent SARS-CoV infection [26]. In confluent virus-infected cells, Akt is first phosphorylated at a single serine residue shortly after SARS-CoV infection, and subsequently dephosphorylated during the course of viral infection [27], whereas Akt, which is ordinary phosphorylated at a serine residue, was dephosphorylated by SARS-CoV infection without any upregulation of its phosphorylation in subconfluent cells [28]. This downregulation of Akt phosphorylation induces inhibition of cell proliferation by SARS-CoV infection and weak activation of Akt cannot induce escape from SARS-CoV-induced apoptosis. Nucleocapsid protein, X1 and spike proteins of SARS-CoV are able to induce apoptosis in their expressing cells [29–32]. Especially, N protein is able to upregulation of phosphorylation of JNK and p38 MAPK, but not ERK and Akt [29]. Although ERK was shown to be phosphorylated in SARS-CoV-infected cells [25], the function is not clear. p90RSK is a well-known substrate for ERK as described above.

In the present study, we showed that Ser380 of p90RSK, which is thought to be auto-phosphorylated after activation of the C-terminal kinase domain, is phosphorylated without upregulation of Thr573 phosphorylation in the C-terminal kinase domain, in SARS-CoV-infected Vero E6 cells. Furthermore, we demonstrated that activation of p38 MAPK was responsible for phosphorylation of Ser380 in virus-infected cells. These results indicated signaling pathways, which are different from those induced by growth factor, contribute to phosphorylation of p90RSK in SARS-CoV-infected cells.

2. Materials and methods

2.1. Cells and virus

Vero E6 cells were subcultured routinely in 75-cm^3 flasks in Dulbecco's modified Eagle's medium (DMEM; Sigma, St. Louis, MO, USA) supplemented with 0.2 mM L-glutamine, 100 units/ml penicillin, 100 μg/ml streptomycin, and 5% (v/v) fetal bovine serum (FBS), and maintained at 37 °C in an atmosphere of 5% CO_2. For use in the experiments, the cells were split once onto 6- and 24-well tissue culture plate inserts and cultured under subconfluent and confluent conditions. SARS-CoV, which was isolated as Frankfurt 1 and kindly provided by Dr. J. Ziebuhr, was used in the present study. Infection was usually performed at a multiplicity of infection (m.o.i.) of 10. The number of cells was counted using the WST-1 cell proliferation assay system (Takara, Shiga, Japan).

2.2. Inhibitor

The p38 MAPK inhibitor, SB203580, which was purchased from Calbiochem (La Jolla, CA, USA), was dissolved in dimethyl sulfoxide (DMSO) at a concentration of 10 mM. The same volume of DMSO alone was used as a control. As shown in previous reports [24,27], SB203580 and PD98059 had no effect on viral replication including viral protein synthesis.

2.3. Western blotting

The whole-cell extracts were electrophoresed on 5–20% gradient polyacrylamide gels, and transferred electrophoretically onto PVDF membranes (Immobilon-P; Millipore, Bedford, MA, USA). In the present study, we applied two sets of samples to polyacrylamide gels, and the membranes were divided into two halves after blotting using

a LumiGLO Elite chemiluminescent system (Kirkegaard and Perry Laboratories, Gaithersburg, ML, USA). When it was necessary to strip the membranes, Restore Western blot stripping buffer (Pierce, Rockford, IL, USA) was used. The following antibodies, obtained from Cell Signaling Technology Inc. (Beverly, MA, USA), were used in the present study at a dilution of 1:1000: rabbit anti-phospho Akt (Ser473) antibody, rabbit anti-Akt antibody, rabbit anti-phospho-PDK1 (Ser241) antibody, rabbit anti-phospho STAT3 (Tyr-705) antibody, rabbit anti-p38 MAPK (Thr180/Tyr182) antibody, rabbit anti-p38 MAPK antibody, rabbit anti-phospho-ERK1/2 (Thr202/Tyr204) antibody, rabbit anti-ERK antibody, rabbit anti-phospho-MEK1/2 (Ser217/221) antibody, rabbit anti-MEK1/2 antibody, rabbit anti-p90RSK1/2/3 antibody, rabbit anti-cleaved Caspase-3 (Asp175) antibody, rabbit anti-cleaved Caspase-7 (Asp198) antibody. Rabbit Mouse anti-STAT3 antibody (diluted 1:2500) was obtained from BD Biosciences (Franklin Lakes, NJ, USA). Rabbit anti-p90RSK1 monoclonal antibody, which was purchased from Epitomics, Inc. (Burlingame, CA, USA), was diluted at 1:1000. Rabbit anti-p90RSK2 (C-term), p90RSK3 (Mid) and p90RSK4 (N-term) were purchased from Zymed Laboratory, Inc. (South San Francisco, CA, USA). Anti-p90RSK2 and 4 antibodies were diluted 1:250, and anti-p90RSK3 was diluted 1:500. Rabbit anti-PARP p85 fragment antibody was purchased from Promega (Madison, WI, USA) and diluted 1:100. Mouse anti-β-actin antibody was purchased from Sigma (St. Louis, MO, USA) and used at a dilution of 1:5000. Rabbit anti-SARS N and M antibodies were described previously [24]. K562 and Jurkat cell lysates were purchased from Clontech Laboratories Inc. (Mountain View, CA, USA).

3. Results

3.1. Signaling pathways in SARS-CoV-sensitive cell lines

As shown in Fig. 1, SARS-CoV-infected confluent Vero E6 cells induced phosphorylation or dephosphorylation of signaling pathways as also described in previous studies [24,27,28]. The cytopathic effects (CPEs) were observed in Vero E6 cells at 24-h post-infection (h.p.i.). DNA fragmentation as an indicator of apoptosis was detected at 24 h.p.i. [24]. Among the signaling pathways activated by SARS-CoV infection, p38 MAPK is thought to act as a pro-apoptotic signaling pathway, whereas Akt has an anti-apoptotic effect. Vero cells, the parental cells of Vero E6, are also sensitive to SARS-CoV infection. However, the time point of the appearance of CPE on Vero cells by SARS-CoV infection is later than that of Vero E6 cells at 24 h.p.i. (data not shown). As shown in Fig. 1A, nucleocapsid (N) protein of SARS-CoV was detected at 17 h.p.i. in both cell lines. The level of N protein in Vero cells was only slightly lower than that in Vero E6 cells, indicating that replication of SARS-CoV is not markedly different between the two cell lines. Anti-apoptotic Akt was phosphorylated at 17 h.p.i. in both cell lines, and was dephosphorylated at 27 h.p.i. (Fig. 1B). Our previous study indicated that phosphorylation level of Akt around 17 h.p.i. is only 20% of phosphorylated Akt in growing cells [28]. Therefore, this low level of activation cannot prevent apoptosis by SARS-CoV infection. Fig. 1B also shows that ERK was phosphorylated at 17 h.p.i. in both cell lines, similar to the observations regarding Akt. The apoptotic markers, PARP (p85) and cleaved caspase-3 and -7, were detected in Vero E6 and Vero cells at 27 and 44 h.p.i., respectively (Fig. 1A). The p38 MAPK in virus-infected Vero E6 and Vero cells was phosphorylated at 17 and 27 h.p.i., respectively (Fig. 1A). Tyrosine of STAT3 was also dephosphorylated via phosphorylation of p38 MAPK as reported previously [25]. Thus, SARS-CoV-induced apoptosis related to time-dependent activation of the pro-apoptotic signaling pathway, p38 MAPK. Taken together, these results suggested that substrates
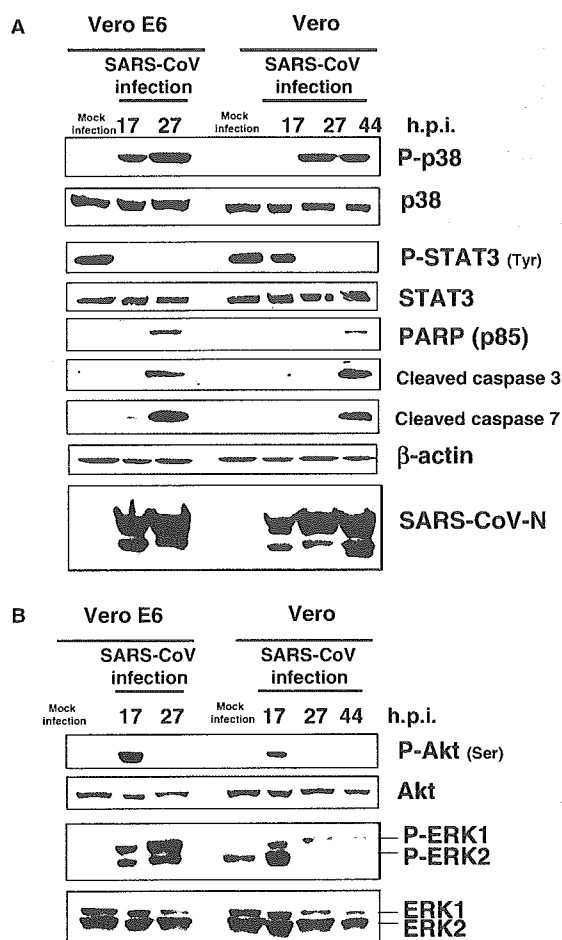
Fig. 1. Phosphorylation of signaling pathways in SARS-CoV-infected cells. Vero and Vero E6 cells were prepared at confluence in 24-well plates and the cells were infected with SARS-CoV at 10 m.o.i. Protein samples were obtained at 17, 24, and 44 h.p.i. The protein of Vero E6 cells at 44 h.p.i. could not be obtained due to strong morphological changes caused by apoptosis. Western blotting analyses were performed to examine signaling pathways (A) and apoptotic marker proteins (B).

Fig. 2. p90RSK family expressed in Vero E6 cells. Vero E6 cells were prepared at densities of 1×10^6 and 0.6×10^5 in 6-well plates. HeLa cells, a clonal cell line for another study, were used as controls. Both K562 and Jurkat cell lysates were obtained from Clontech Laboratories Inc. Western blotting analysis was performed using the same amounts of protein. According to the antibody product data sheets, anti-human p90RSK1 monoclonal antibody (Epitomics) does not cross-react with other RSK family members. Anti-human and mouse p90RSK2 antibody (Zymed) does not react with overexpressed p90RSK1, 3, or 4. Anti-human p90RSK3 antibody (Zymed) does not react with overexpressed p90RSK1, 2, or 4. Anti-human p90RSK antibody (Zymed) does not react with p90RSK1, 2, or 3. Anti-p90RSK1/2/3 antibody (Cell Signaling) detects endogenous levels of RSK1, RSK2, and RSK3 proteins. In Vero E6 cells, the band of RSK1 was stronger than that of RSK2 as described in the text. The weak bands were enhanced using Adobe Photoshop.

of PI3K/Akt, ERK1/2, and p38 MAPK are important for understanding the cytopathic effects of SARS-CoV infection.

3.2. Phosphorylation of p90RSK Ser221 in Vero E6 cells

p90RSK is phosphorylated by both PDK-1 and ERK [2,13,14]. Ser221 of p90RSK1 is phosphorylated by PDK-1 and Thr359, Ser363, and Thr573 of p90RSK-1 are phosphorylated by ERK. p90RSK is thought to play important roles in apoptosis and the cell cycle. Both PI3K/Akt and ERK signaling pathways are activated early post-infection with SARS-CoV in both Vero and Vero E6 cells (Fig. 1B). Therefore, p90RSK may be a target of both signaling pathways in SARS-CoV-infected cells. At least four species of p90RSK (p90RSK1, 2, 3, and 4) has been reported to date [2–5]. We used anti-p90RSK antibodies, which do not cross-react with other p90RSK family members, as described in the legend of Fig. 2. We measured densities of RSK1 and 2 bands in Vero E6 cells using LAS-3000 mini system (Fuji Photo Film Co.
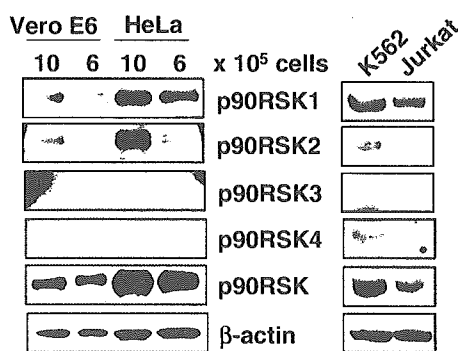
Ltd, Tokyo, Japan). The amount of p90RSK1 in subconfluent cells, p90RSK2 in confluent cells and p90RSK2 in subconfluent cells were 73.05%, 39.94% and 14.70% of RSK1 in confluent cells, respectively. Although affinity of each antibody is different, this result suggested that p90RSK1 was expressed stronger than p90RSK2 in Vero E6 cells. p90RSK1 is expressed mainly in the human kidney, lung, and pancreas, whereas p90RSK2 is expressed in skeletal muscle, heart, and pancreas [33]. p90RSK3 and 4 were not detected in Vero E6 and HeLa cells in the present study. The p90RSK4 was weakly detected in K562 and Jurkat cells.

We examined the phosphorylation status of p90RSK Ser221 in Vero E6 cells. Our previous study indicated that very low levels of Akt in confluent Vero E6 cells are phosphorylated at serine, whereas the level is high in subconfluent cells [28]. However, the phosphorylated threonine of Akt is difficult to detect in subconfluent Vero E6 cells. We only detected it weakly when the cells were treated with epidermal growth factor (EGF) at 1 min [28]. As threonine of Akt was transiently phosphorylated by EGF treatment, it was never detected after 5 min. On the other hand, serine of Akt was easily phosphorylated by treatment with EGF after 3 min. The threonine residue of Akt is phosphorylated by PDK-1, and the serine residue of Akt is thought to be phosphorylated by the putative kinase, PDK-2. To compare the phosphorylation level of PDK-1 at different cell densities, Vero E6 cells were prepared at 10, 5, 2.5, 1.25, 0.6, and 0.3×10^5 cells in 5% FBS containing DMEM per well in 6-well plates. At a density of 10×10^5 cells, Vero E6 cells showed 100% confluence in this experiment. As shown in Fig. 3A, the level of PDK-1 phosphorylation was similar at all cell densities. Ser221 of p90RSK was also phosphorylated at a similar level. The confluency of Vero E6 cells in the present study is shown in Fig. 3B. To confirm that the
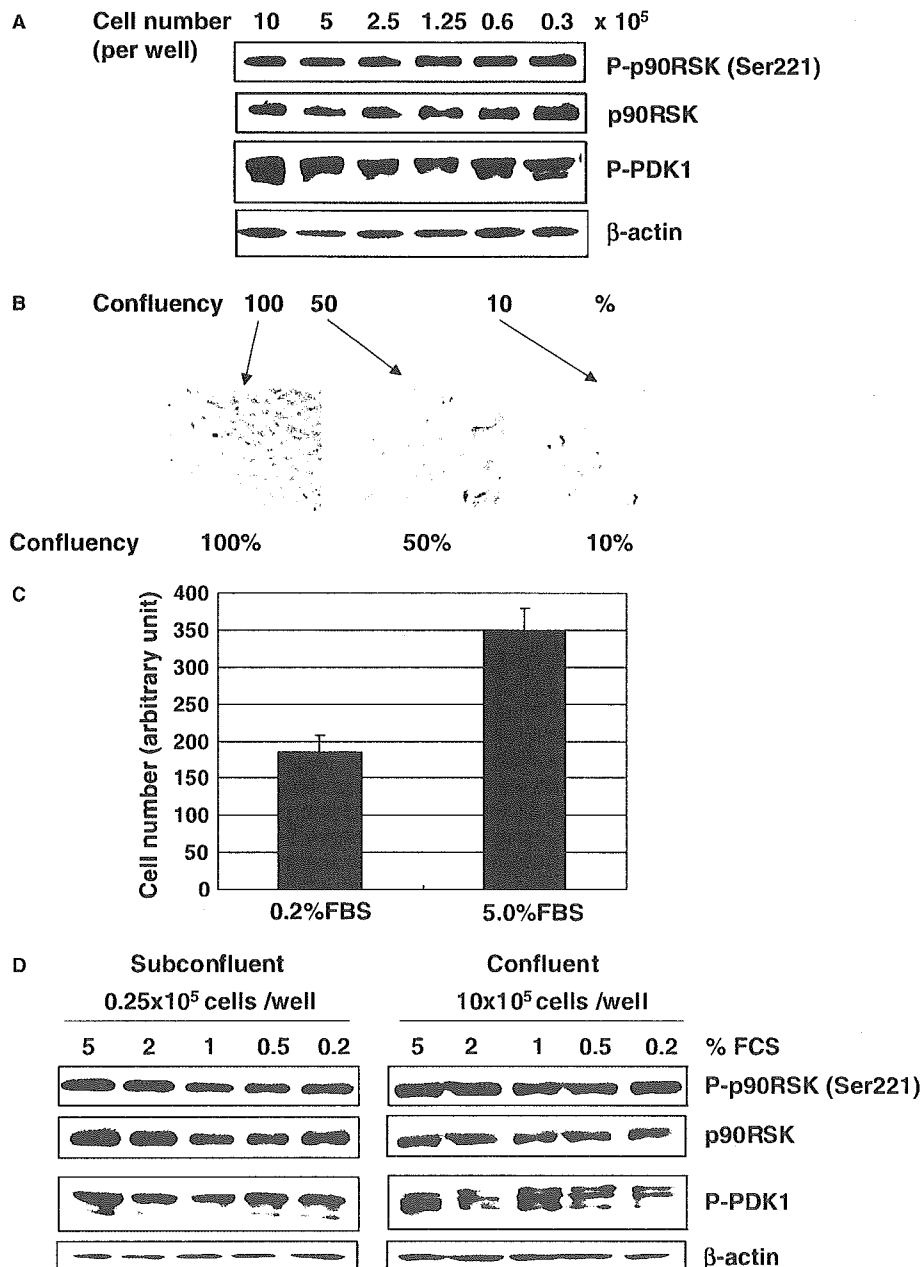
A Cell number 10 5 2.5 1.25 0.6 0.3 x 10^5
(per well)

P-p90RSK (Ser221)

p90RSK

P-PDK1

β-actin

B Confluency 100 50 10 %

Confluency 100% 50% 10%

C

D Subconfluent   Confluent
0.25x10^5 cells /well   10x10^5 cells /well

| 5 | 2 | 1 | 0.5 | 0.2 | | 5 | 2 | 1 | 0.5 | 0.2 | % FCS |

P-p90RSK (Ser221)

p90RSK

P-PDK1

β-actin

Fig. 3. Phosphorylation of p90RSK Ser221 in Vero E6 cells. (A) Vero E6 cells were prepared at densities of 10, 5, 2.5, 1.25, 0.6, and 0.3×10^5 cells in DMEM containing 5% FBS per well in 6-well plates. Proteins were obtained from these cells after 24 h, and Western blotting was performed using anti-phospho p90RSK (Ser221). (B) The confluency of Vero E6 cells used in this study is shown. (C) 2×10^3 cells in DMEM containing 0.2% and 5% FBS were prepared in 96-well plates. After 4 days, cell number was counted using a WST-1 cell proliferation assay kit. (D) 0.25 and 10×10^5 cells in DMEM containing various concentrations of FBS were prepared in 6-well plates. Western blotting was performed using proteins obtained after 24 h.

phosphorylation levels of PDK-1 and p90RSK Ser221 were unaffected by cell proliferation, Vero E6 cells were cultured in medium containing low and high concentrations of FBS. Cell proliferation of Vero E6 cells was partially suppressed in medium containing 0.2% FBS as compared with 5% FBS (Fig. 3C). Confluent and subconfluent cells in medium containing 5–0.2% FBS showed similar phosphorylation levels of PDK-1 and p90RSK at Ser221 (Fig. 3D). Thus, the phosphorylation level of Ser221 of p90RSK is not influenced by the status of cell proliferation.

3.3. Phosphorylation of p90RSK Ser380 and Thr573 in Vero E6 cells

p90RSK1 is phosphorylated at Thr573 in the activation loop of the C-terminal kinase domain [9,10], and this activation of the C-terminal kinase domain is thought to lead to autophosphorylation at Ser380 [11]. Activation of the C-terminal domain by the ERK signaling pathway is thought to be necessary for phosphorylation at Ser380 [34]. Fig. 4A indicates that EGF treatment induces phosphorylation of ERK in Vero E6 cells. Both Thr573 and Ser380 of p90RSK were phosphor-

ylated early after EGF treatment. Interestingly, the phosphorylation level of p90RSK Ser221 was not altered by EGF treatment. To investigate whether cell density affects phosphorylation level of p90RSK Thr573 and Ser380, Western blotting analysis was performed using proteins obtained from 10, 5, 2.5, 1.25, 0.6, and 0.3×10^5 cells in DMEM containing 5% FBS per well in 6-well plates. Fig. 4B shows that Ser380 of p90RSK phosphorylation was increased by decreasing cell density. Although Thr573 was also increased phosphorylation by decreasing cell density, the amount was very low. The amount of Thr573 phosphorylated p90RSK in 0.3×10^5 cells is only 11.53% of Ser380 using LAS-3000 mini system. Therefore, the band of Thr573 phosphorylated p90RSK was difficult to see in Fig. 4B.

3.4. Phosphorylation of p90RSK in SARS-CoV-infected cells

To investigate regulation of p90RSK phosphorylation in SARS-CoV-infected cells, confluent Vero E6 cells were infected with SARS-CoV at approximately 50 m.o.i., and Western blotting analysis was performed using proteins at 26 and 24 h.p.i. As shown in Fig. 5A, no significant differences in phosphorylation levels of PDK-1 or p90RSK at Ser221 were observed between confluent virus-infected cells at 16 and 24 h.p.i. Phosphorylation of Thr573 was not upregulated by viral infection. Ser380 of p90RSK is phosphorylated in virus-infected confluent cells. Previous reports indicated autophosphorylation of Ser380 after activation of C-terminal kinase domain [11]. Thus, phosphorylation of p90RSK Ser380 is upregulated without upregulation of Thr573 in SARS-CoV-infected cells.

3.5. Phosphorylation of p90RSK Ser380 under ERK and p38 MAPK signaling pathways

These observations raise a question regarding which signaling pathway regulates phosphorylation of Ser380 of p90RSK in SARS-CoV-infected cells. p90RSK is thought to act in response to stimulation and p38 MAPK plays key roles in cytopathic effects in SARS-CoV-infected cells, as shown in Fig. 1 and in our previous study [24]. As shown in Fig. 5A, Ser380 was phosphorylated without phosphorylation of Thr573 in virus-infected cells, suggesting that the ERK signaling pathway is not important for phosphorylation of Ser380. We next investigated whether p38 MAPK inhibitor can inhibit phosphorylation of Ser380. Confluent cells were prepared in 24-well plates. Cells were infected with SARS-CoV for 1 h, and then SB203580 was added as a p38 MAPK inhibitor. Western blotting analysis was performed using proteins at 24 h.p.i. As shown in Fig. 5B, phosphorylation of Ser380 was decreased in SB203580-treated cells.

4. Discussion

In the present study, we showed that p90RSK, the best-known substrate of ERK and PDK-1, was regulated phosphorylation in SARS-CoV-infected Vero E6 cells. There has been one previous report regarding phosphorylation of p90RSK by viral infection. Rous sarcoma virus has the ability to phosphorylate p90RSK [35], but there have been no detailed analyses of p90RSK phosphorylation. Investigation of the phosphorylation status of p90RSK by viral infection is
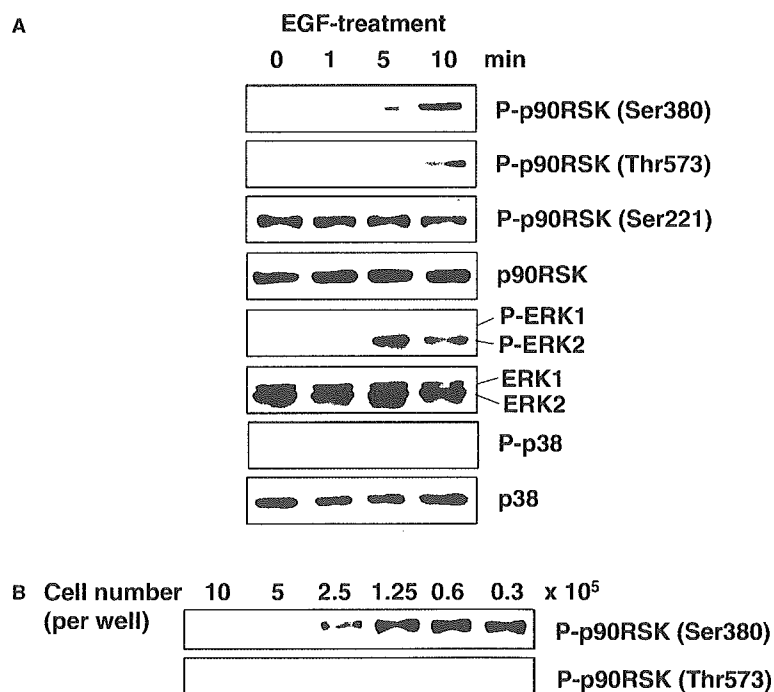

Fig. 4. Phosphorylation of p90RSK Thr573 and Ser380 in Vero E6 cells. Confluent Vero E6 cells in 24-well plates were treated with EGF. Western blotting analysis was performed using proteins obtained at 0, 1, 5, and 10 min (A). (B) Vero E6 cells were prepared at 10, 5, 2.5, 1.25, 0.6, and 0.3×10^5 cells in 6-well plates. Proteins were obtained from these cells after 24 h, and Western blotting was performed using anti-phospho p90RSK (Thr573 and Ser380). The proteins used in (B) were the same as those in Fig. 3A, and equal amount of proteins were blotted.